A FACTS Based Hybrid Filter Compensator (HFC) for H2V Battery Charging Schemes

E. Elbakush*‡, A. M. Sharaf**

*Department of Electrical and Computer Engineering, University of New Brunswick

**Energy Research Center-SSE-Habib University

e.elbakush@unb.ca, profdramsharaf@yahoo.ca

‡ Corresponding Author; E. Elbakush, 15 Dineen Dr., D36 Head Hall, +1506471 9589, e.elbakush@unb.ca

Received: 29.01.2013 Accepted: 24.03.2013

Abstract- The paper presents a robust low impact FACTS based filter compensation scheme for V2H Battery chargers to, improve the power quality, reduce total harmonic distortion, decrease AC and DC inrush currents, and ensure effective Ac and DC Common bus voltage stabilization. The Neutral point Facts Filter Compensation Schemer (NP-HFC) ensures effective decoupling of the AC-DC Sides and minimal impact of inrush currents during fast charging modes. In the same time, the novel FACTS device ensures efficient energy utilzation and improved power factor at the common AC bus. A dynamic multi regulation multi-loop error driven control strategy is developed to ensure fast charging, minimal impact on host electric grid and efficient utilization of grid-connected battery charging scheme with effective AC-DC decoupling and stabilization of the DC Common Bus Voltage. The self regulating battery charging multi- regulator control scheme has been fully validated using Matlab-Simulink Software Environment. The FACTS-based Battery Charging V2H unit is controlled using modified multi-zonal error driven control strategies for fast dynamic action and minimal stead state error to ensure improved power factor operation, reduced Total Harmonic Distortion and decoupled AC- DC Grid Operation. The battery charger has a hybrid selected Voltage-Current Regulation strategy.

Keywords- Electric Vehicle, FACTS NP- HFC, Multi-zonal Intercoupled Controller, V2H Battery Charger.

1. Introduction

Electrical Vehicle charging systems are infrastructures and equipment which provide power supply to power battery of electric vehicle, mainly including battery exchange station and charging pole and charging station. The V2H system can quickly charge an EV with direct current from the storage battery, and can supply the electricity in the EV back to the household.

There are massive ranges of both social and economic benefits driving the introduction of Electric Vehicles (EVs). These benefits include an improvement of air quality, a reduced dependency on oil supplies, a reduction of traffic noise, an enhanced capacity to decrease greenhouse gas emissions and potential economic savings. EVs have particular potential to transform the transport industry because they introduce electricity as a possible vehicular fuel for private transport. The concerns about the petrol reserves and prices, as well as pollution and global warming issues have increased the interest on electric vehicles. The governments have started to provide more incentives and, private companies have concentrated on electric vehicle development projects [1]

Today's climate and price of energy sources push increasingly towards a diversification of transportation fuels, an improvement in energy efficiency and a decrease in emissions. By using electrical energy for plug-in hybrid electric vehicles (PHEV) and electric vehicles (EVs) will offer the potential to partly fulfill these challenging requirements. Emission reductions and the amount of primary energy conservation due to plug-in vehicles are, however, highly dependent on the energy system. In past ten years of studies, it has seen that, main consideration was concentrated on series and parallel hybrid drives. Lately however, plug-in hybrids (PHEV) and all electric vehicles (EVs) seem receiving more attention. An EV is defined as

any vehicle that utilizes an electric motor to form part of the vehicular drive train. EVs are classified based upon their engine configuration. The three categories are Hybrid Electric Vehicles (HEV), Plug-in Hybrid Electric Vehicles (PHEV) and Battery Electric Vehicles (BEV). PHEVs and BEVs are collectively known as Plug-in Electric Vehicles (PEV) [2], [3].

The automobile industry continues to grow by leaps and bounds, and due to the increase in the number of vehicles worldwide, air-pollution continues to increase. Though the automobile manufacturers have reduced the emission of greenhouse gases such as hydrocarbons, carbon monoxide, carbon dioxide etc., from the vehicles, they cannot produce a zero-emission vehicle unless they produce an electric vehicle (EV) [4].

The electric vehicle is an emission free, environment friendly vehicle. However, the electric vehicles remain unpopular among the consumers due to their lack of performance and their inability to travel long distances without being recharged. So, the general consumers and the environmentalists alike are greatly anticipating vehicles that embrace both the performance characteristics of the conventional automobile and the zero-emission characteristics of the electric vehicles. These lead manufacturers to come up with a vehicle that is acceptable by the consumers and also meets the performance of the conventional vehicle with much less emissions. Such vehicles are branded as Hybrid Electric Vehicles (HEV), the name being derived from their ability to run in either gasoline mode or electric mode or both [5].

The electric motor in the hybrid electric vehicle assists the gasoline engine during acceleration and receives its power from a dedicated battery pack. The beauty of the HEV is that energy can be fed back into the battery for storage, e.g., during regenerative braking (which is otherwise wasted as heat in a conventional vehicle). Leading car manufacturers like Toyota and Honda have already started mass producing HEV cars, Prius and Insight respectively, which are now becoming very popular among the consumers for their incredible mileage and less emissions. In the coming years many more automobile manufacturers will come up with their own HEVs. Currently, the sport-utility vehicles (SUVs) are the largest gas consuming vehicles and one of the most popular vehicles in USA. It will be a great breakthrough if hybrid SUVs come into the market, and it will certainly become a reality in the near future [6], [7].

The industry-standard battery charging approach is to utilize a two-stage AC-DC power convertor with power factor correction (PFC) [8]. The first stage is commonly a buck- boost regulator, which adjusts the DC-link voltage level and the line current waveform, and the second stage is one of the different types of DC-DC converters [9]. The AC-DC front-end is the most important part of the battery charger, and it is necessary to select the topology, which fulfills the regulatory requirements of input current harmonic and power factor correction. The most common topology for battery chargers is a boost one for PFC application, which uses a diode bridge as an AC/DC rectifier followed by a buck-boost section [10-12].

Dynamicall controlled FACTS devices have been proposed to eliminate line current harmonics, improve power factor, and increase power quality. In this paper, a novel Hybrid Filter Compensator HFC is proposed and utilized in a buck-boost converter for plug-in hybrid electric vehicles. The proposed FACTS- based device is a member of a Family of V2H and V2G devices and controlled by a quad-loop Multi-zone Dynamic Controller. In order to achieve the best charging performance, a quad-loop error-driven controller is also designed for DC-DC buck-boost chopper. Digital simulation is used to compare the operation of the mobile/EV battery charger without and with HFC FACTS device for harmonic reduction, power factor correction, and power quality improvement [13], [14].

2. System Description

The basic battery charge without inter-coupled Hybrid Filter Compensator (HFC) FACTS scheme and the proposal scheme are shown in Figures (1-2) respectfully, which consist of a full wave bridge rectifier that is used to convert the AC supply voltage form to DC form. This DC voltage is stepped up using DC-DC Buck-boost converter. Battery powered systems often stack cells in series to achieve higher voltage. Nevertheless, sufficient stacking of cells is not possible in many high voltage applications due to lack of space. Buck-boost converters can increase the voltage and reduce the number of cells. As seen the scheme, there is free-wheeling diode that has been connected in reverse direction and in parallel with the loads. This diode helps in providing a smooth current to the load and also eliminates the negative voltage across the load. The switching ON and OFF of the DC-DC Buck-boost converter switch (SA and SB) is achieved by a pulse signal generated from Pulse-Width Modulation (PWM). The modulating signal of PWM is generated from Multi-Loop Weighted Modified SMC Sliding mode controller. The output of DC-DC Buck- boost converter is used to charge a high ampere-hour battery.

The Neutral Point Hybrid Filter Compensator (NP-HFC) is connected in parallel with the full wave rectifier to eliminate line current harmonics, improve power factor, and increase power quality. The Neutral Point Hybrid Filter Compensator (NP-HFC), shown in Figure (2), is a combination of two shunt capacitors with a tuned arm shunt filter. The switch (SC) is controlled by switching pulses (P1) that is generated by PWM, as shown in Figure (2).

The FACTS (NP-HFC) filter topology can be changed by the complementary switching PWM pulses as follow:

Case 1: If pulse (P1) is high and (P2) is low, the resistor and inductor will be disconnected and the shunt capacitor will provide the required shunt capacitive compensation to the AC system to improve the power factor.

Case 2: If pulse (P1) is low and then (P2) is high, the resistor and inductor will be connected into the circuit as a tuned arm filter to mitigate the harmonics.

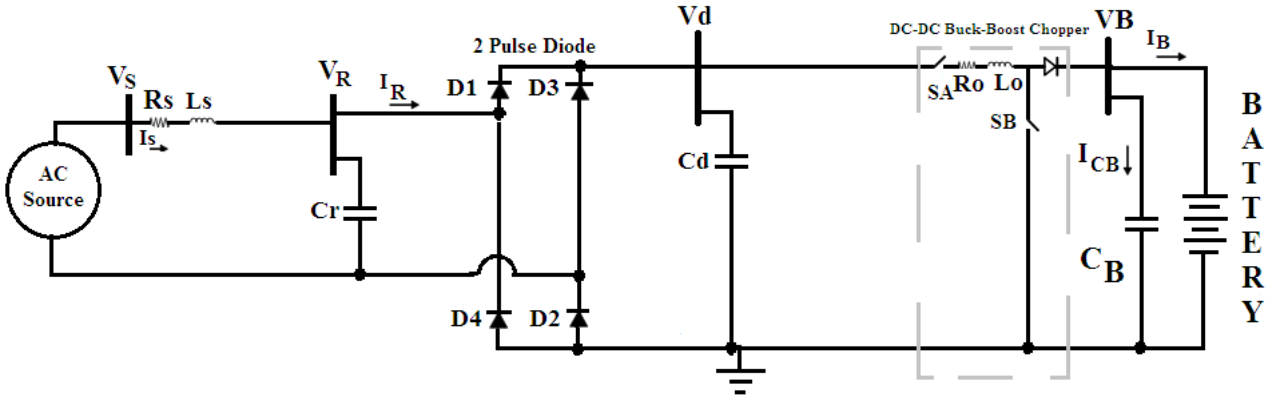

Fig. 1. Basic Scheme For Electric Vehicles with no NP-HFC.

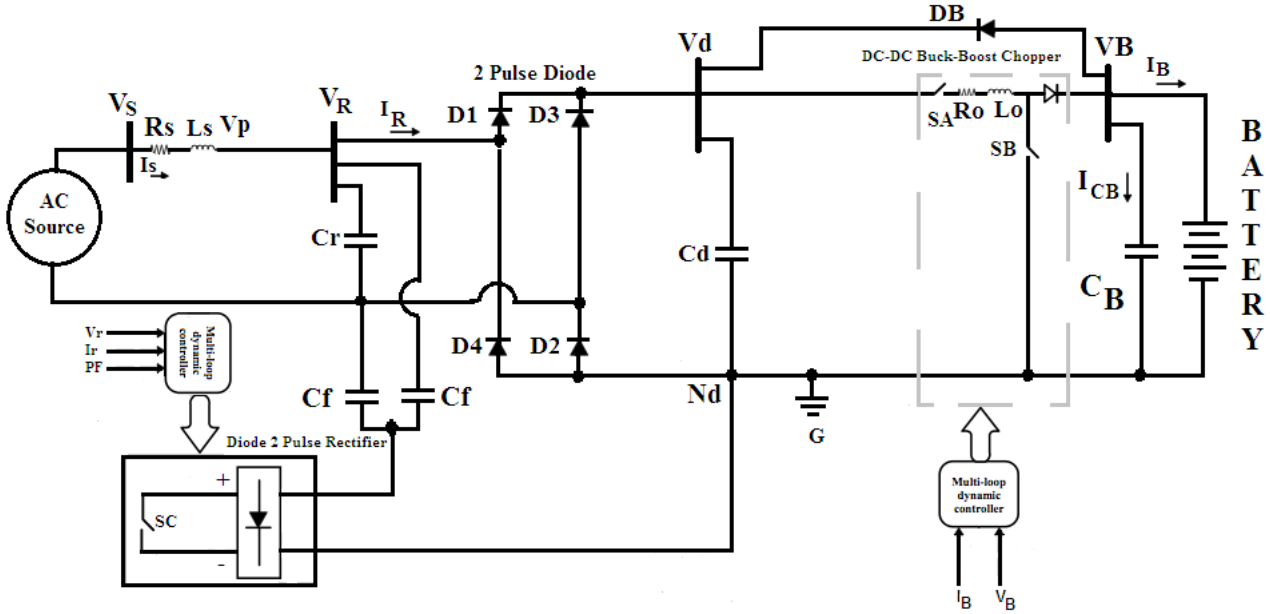

Fig. 2. Proposed FACTS Based (NP-HFC) V2H-Battery Charging Scheme For Electric Vehicles.

3. Multi-Zone Dynamic Controller

The novel Tri-loop error driven multi-zonal dynamic dynamic target practice controller is implemented to stabilize the common AC and DC Buses. The dynamic regulation loops ensure energy efficient utilization and reduced current ripple content.

The multi-zonal dynamic controller parameters and zonal boundaries can be optimized offline to provide a robust, parameter insensitive and external disturbance tolerant feature as well as fast dynamic response and structure simplicity in implementation of hardware [15], [16]. The global error signal is an input to the Multi-zonal dynamic controller to regulate the modulating control signal to the PWM switching block as shown in Figure (3). Multi-zonal dynamic controller includes error sequential activation supplementary loops to ensure fast dynamic response and affective damping of large excursion. The dynamic quad-loop controller includes two main loops and two sub-loops Figures (5 - 6). The main loops function as tracking the errors of the values of voltages and currents of both buses on DC and AC sides of the diode bridge. Moreover, the sub-loops function as tracking the errors of the ripples of voltages and currents of both buses on DC and AC sides of the diode bridge. All the values of scaling and time delay of the controller were selected by an offline guided trial and error method to insure fast response and minimum total error [17].

The novel tri-loop regulation scheme can compensate for any sudden, inrush and dynamic changes and excursion in bus voltage and motor current at the common DC- bus. The loop weighing factors are assigned to ensure loop decoupling with a dominant voltage stabilization loop. The total error signal is used to ensure dynamic power utilization using an error scaling signal Re which represents the input to multi zone controller to adjust the Pulse Width Modulated (PWM) generator through a limiter as shown in Figures (5 - 6) for both NP-HFC and buck-boost DC- DC chopper. The dynamic control-error scaled actor Re is related to the total error value by the following error-excursion vector magnitude scaled equation:

$$R_e = Sqrt((\frac{de_t}{dt})^2 + (e_t)) \quad (1)$$

The novel dynamic tri-loop control strategy is essentially a successive dynamic error driven regulator. The dynamic controller is insensitive to sudden excursions and torque variations. The selected absolute error range and the number of control zones are optimized off line by minimizing an absolute error scaled objective function. The absolute range of Re and the corresponding control signal are indicated in Table (I). Zonal Activation Target Practice Controller is composed from concentric circles representative zones, each circle has a radius depends on the values of the total error and the first derivative of the total error as shown in Figure (4). Figure (3) shows Multi-zone dynamic controller controls a dynamic quad-loop error driven controller. This Multi-zone dynamic controller has an additional Error-Squared loop that would be added to the output of the conventional Multi-zone dynamic controller provides an input signal for a Pulse Width Modulation block (PWM) to adjust PWM reference voltage (modulating voltage), and it is compared with a fixed carrier signal. Then, a pulsing/switching sequence would be produced to turn on the complementary IGBT switches. By switching sequence, the equivalent admittance of the filter is modulated [18], [19]. Multi-zone dynamic controller is validated for voltage stabilization and dynamic reactive compensation using Matlab/ Simulink/SimPower Toolbox software environment.

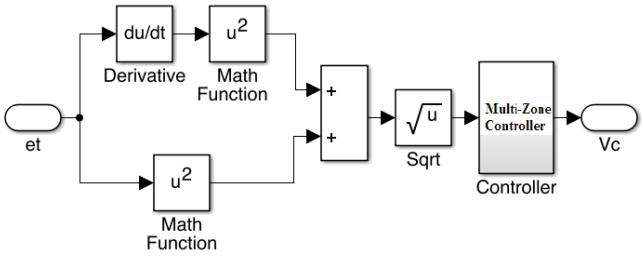

Fig. 3. Dynamic error driven Multi Zonal Controller.

TABLE I
SELECTED ZONES AND CONTROL SIGNAL ASSIGNMENT

Zone No.	Re Range pu	Control signal Vc pu
1	0<Re> 0.02	0
2	0<Re> 0.05	0.10
3	0<Re>0.10	0.20
4	0<Re> 0.15	0.25
5	0<Re> 0.20	0.30
6	0<Re> 0.25	0.40
7	0<Re> 0.30	0.45
8	0<Re> 0.35	0.50
9	0<Re> 0.40	0.55
10	0<Re> 0.50	0.60
11	0<Re> 0.60	0.70
12	0<Re> 1.00	1.00

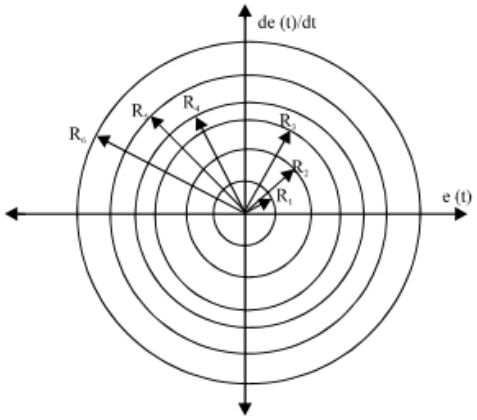

Fig. 4. Zonal activation target Controller.

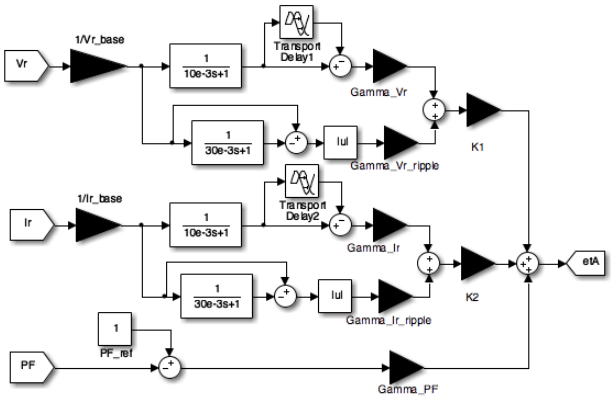

Fig. 5. Dynamic Tri-Loop Regulator A for the AC HFC Filter Compensator.

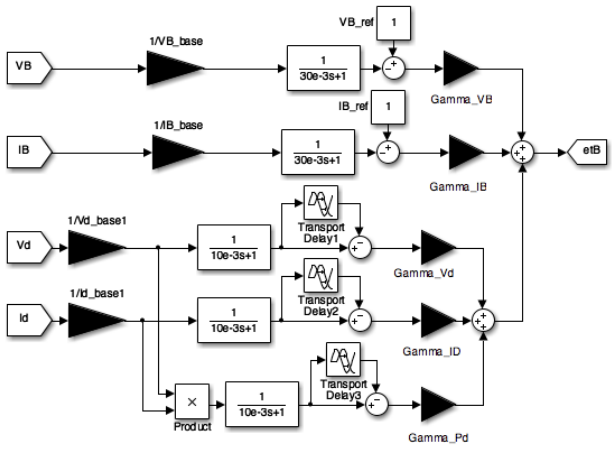

Fig. 6. Dynamic Tri-Loop Regulator B for buck-boost DC-DC Battery charging chopper.

4. Lithium Battery

Lithium-ion (Li-ion) batteries are an attractive proposition for use in high-performance electric vehicles. In comparison with other rechargeable batteries, Li-ion provides very high specific energy and a large number of charge/discharge cycles. The cost is also reasonable. Thus, Li-ion batteries are the preferred choice over other

technologies such as silverzinc and nickelmetal-hydride. Presently, however, Li-ion batteries are only commercially available in small sizes. Accordingly, large numbers of cells have to be assembled in series/parallel configurations to achieve the desired battery sizes. This, combined with safety issues, presents the challenge of making highly efficient, highly reliable, battery packs for use in electric vehicles [20], [21]. The charge and discharge of a rechargeable Lithium-ion battery are very complicate electro- chemical process, which has been modeled and analyzes mathematically from the electro-chemical point of view. The Figure (7) shows The Rechargeable Lithium-ion battery. The models are more precise because the equations are derived from the internal chemical reaction of Lithium-ion batteries. The measured battery voltage at the terminals Vbat is model as the sum of the battery electro-motive force (EMF) and the product of the current and the equivalent over-potential resistance at the instant of time as shown in Eq. (2).

$$EMF(SOC) = V_{bat}(t) - i(t) \times R_{overpotential}(SOC) \quad (2)$$

The battery EMF is highly related to the State of Charge (SOC) of the battery and there are several methods to measure the EMF of the battery directly or indirectly [22], [23]. The method we adopted is the voltage relaxation method which charges and discharges the battery with a small current rate then relax (rest) for a period of time to let the battery reach the equilibrium state.

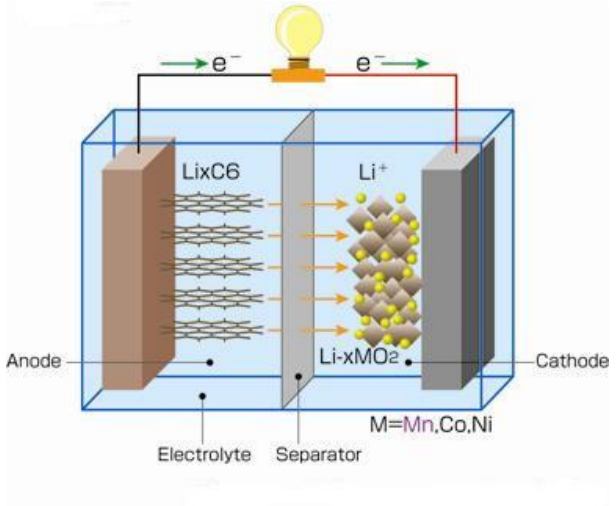

Fig. 7. Rechargeable Lithium-ion Battery.

5. Proposed NP-HFC FACTS-Based Active Power Filter

The Neutral Point Hybrid active filters have been presented in the literature as a lower cost alternative to purely active filters for harmonic compensation. The Neutral Point Hybrid filters use combinations of passive elements to reduce the ratings of the active element required [24], [25]. The development of hybrid filter topologies has followed a natural progression from purely passive tuned filters, which have been used for many years, to simplified passive structures with one active element. These passive structures have been largely based on the original tuned structures.

In order to enhance the inter-coupled AC-DC FACTS based low impact battery charging scheme For Electric Vehicles system performance a NP-HFC Filter Compensator comprising switchable capacitor is introduced at the AC and DC buses. The Neutral Point Hybrid Filter Compensator (NP-HFC) is also controlled to absorb ripple and reduce DC side current oscillations. The idea behind the controller is to detect major excursions in the voltage and current measurements and feed the errors to a PWM module that in turn generates the switching pulses to the filter switches in accordance with the duty ratio and the error value [26]. NP-HFC Filter Compensator used and tested with the operation of charging electric vehicles is shown in Figure (2).

The Neutral Point Hybrid Filter Compensator control scheme is based on a decoupled current and voltage components of the DC bus. The NP-HFC Filter Compensator must be connected across the DC bus terminal to maintain constant DC voltage in order to allow operation of the VSC-converter with two control loops as shown in the Figure (2). The primary duty of the capacitor bank is to provide a voltage path, current path as shown in Figure (5). The input of control loop 1 is the bus voltage, which produces an error with respect to the measured value and then, the error is used for voltage regulation. The input to loop 2 is the bus current that has the same transfer function as the voltage loop [26].

6. Digital Simulation Results

In order to validate the dynamic effectiveness of the inter- coupled NP-HFC and DC-DC Buck-Boost chopper for improving the power quality, the system shown in Figure (2) is simulated using MATLAB/SIMULINK software. In this case, NP-HFC is connected between AC and DC sides of the diode converter and parallel with it as shown in Figure (2). Figures (8 - 15) show RMS voltages and RMS currents for all the Buses. It is clearly observed that the power factor and voltage in the nodes have been improved by using the proposed NP-HFC FACTS device. In the same time, Figures (16 - 22) show Active Power, Reactive Power, and Apparent for all the Buses. It is obvious that the Active Power, Reactive Power, and Apparent for all the Buses have been improved by using the proposed NP-HFC FACTS devices. The power factor at both common interface AC and DC nodes is enhanced to near unity as shown in Figure (23). Figures (24 - 26) show the THD of the Voltage and the Current of the Source Bus and the Battery Bus. It is clearly observed that the THD of the Voltage and the Current have been improved by using the proposed NP-HFC FACTS devices. Figures (46 - 48) show the Fast Fourier Transformation (FFT) harmonic spectra of currents and voltages at AC nodes. The proposed NP-HFC FACTS device decreases the harmonic content on the grid. FFT spectra of the voltages and currents showed reduction in low order harmonic magnitudes. Through dynamic simulation, a short circuit and open circuit faults are applied on Ac side of the rectifier of the AC source as shown in Figures (32- 45). Figures (28 - 29) show V-I-P three-dimensional characteristic at all Buses for the both cases, without and with NP-HFC inter-coupled FACTS devices. The hybrid

multi node Volt-Current-Power weighted charging mode for fast charging current condition and limited Inrush.

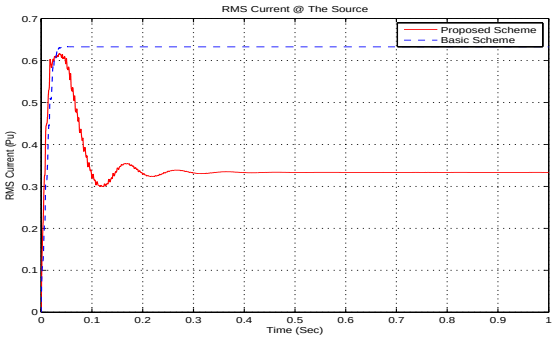

Fig. 8. RMS Current @ Vs Bus with and without NP-HFC Compensator.

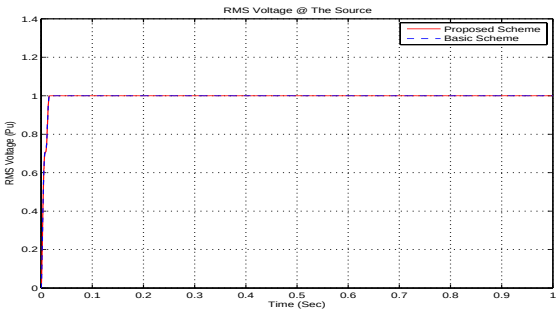

Fig. 9. RMS Voltage @ Vs Bus with and without NP-HFC Compensator.

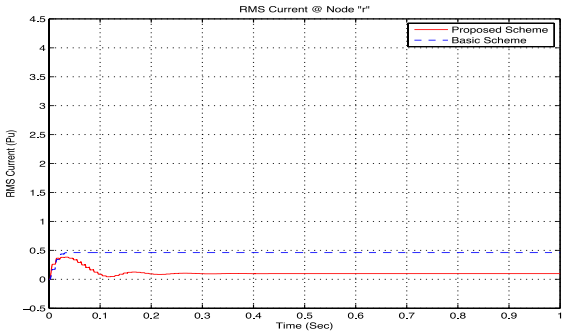

Fig. 10. RMS Current @ Vr Bus with and without NP-HFC Compensator.

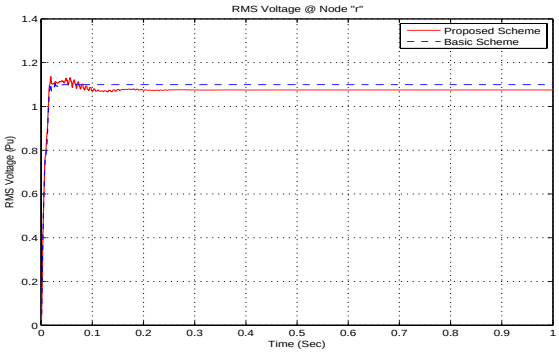

Fig. 11. RMS Voltage @ Vr Bus with and without NP-HFC Compensator.

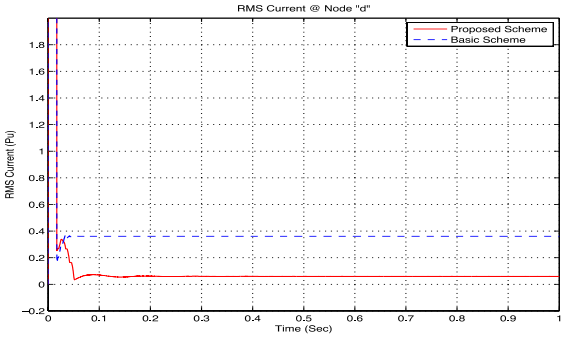

Fig. 12. RMS Current @ Vd Bus with and without NP-HFC Compensator.

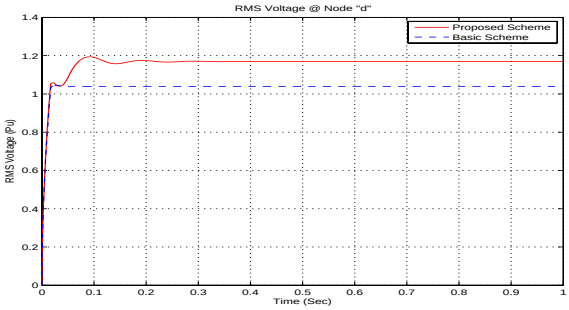

Fig. 13. RMS Voltage @ Vd Bus with and without NP-HFC Compensator.

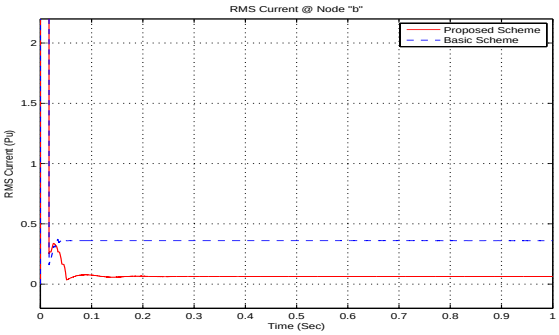

Fig. 14. RMS Current @ Vb Bus with and without NP-HFC Compensator.

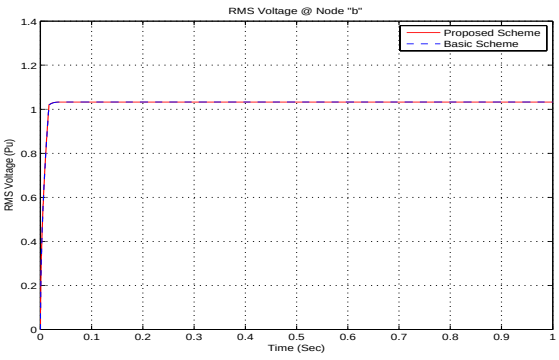

Fig. 15. RMS Voltage @ Vb Bus with and without NP-HFC Compensator.

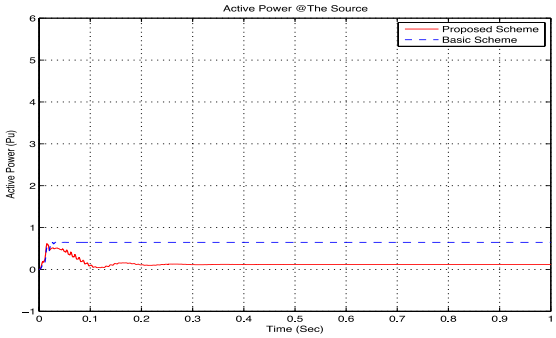

Fig. 16. Active Power @ Vs Bus with and without NP-HFC Compensator.

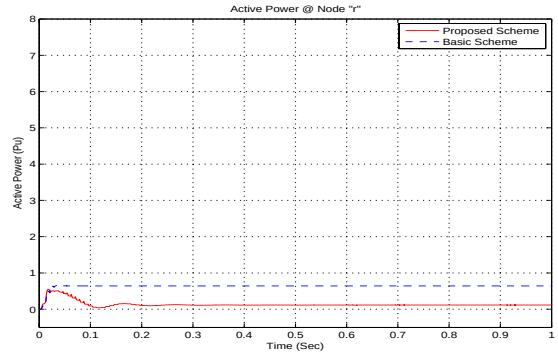

Fig. 17. Active Power @ Vr Bus with and without NP-HFC Compensator.

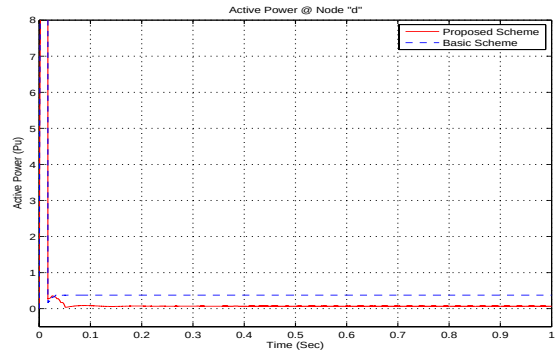

Fig. 18. Active Power @ Vd Bus with and without NP-HFC Compensator.

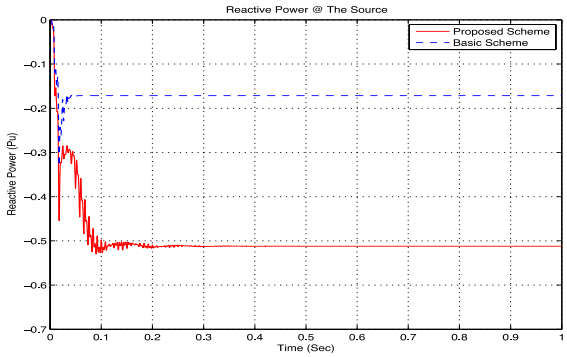

Fig. 19. Reactive Power @ Vs Bus with and without NP-HFC Compensator.

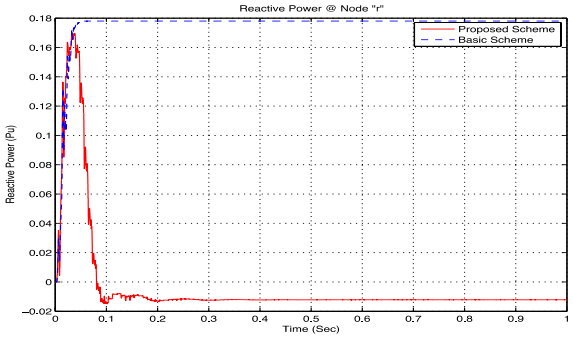

Fig. 20. Reactive Power @ Vr Bus with and without NP-HFC Compensator.

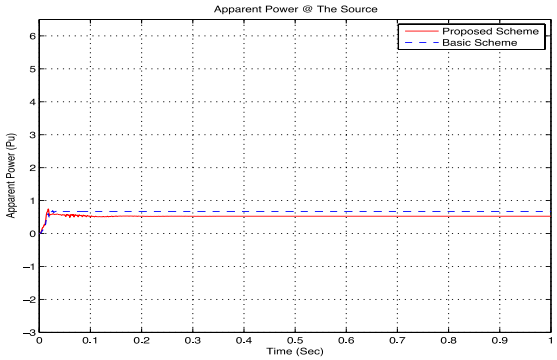

Fig. 21. Apparent Power @ Vs Bus with and without NP-HFC Compensator.

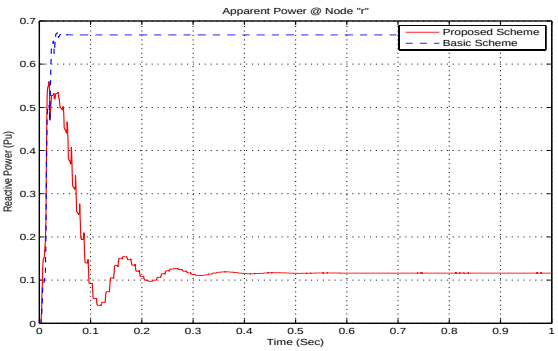

Fig. 22. Apparent Power @ Vr Bus with and without NP-HFC Compensator.

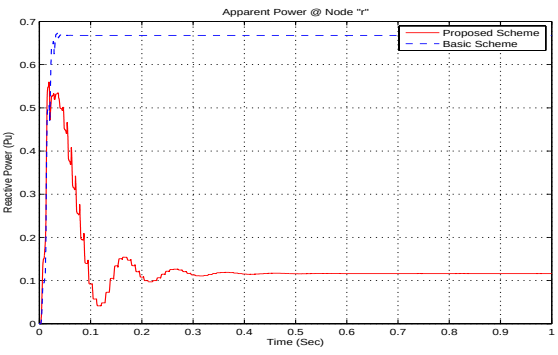

Fig. 23. Power factor @ Vr Bus with and without NP-HFC Compensator.

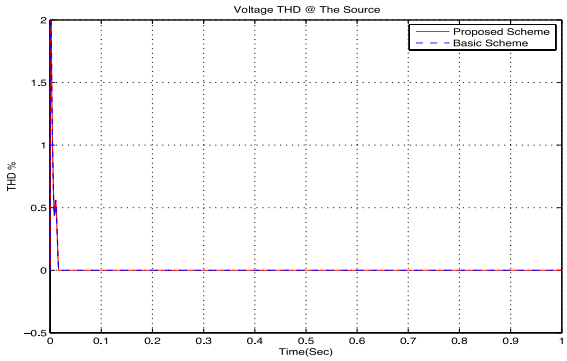

Fig. 24. THD % of the Voltage @ Vs Bus with and without HFC Compensator.

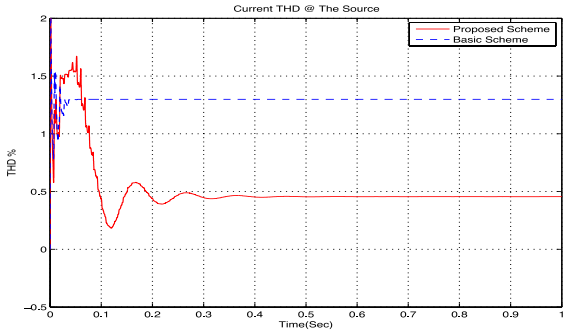

Fig. 25. THD % of the Current @ Vs Bus with and without NP-HFC Compensator.

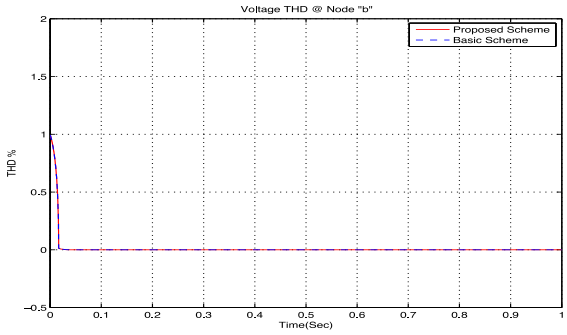

Fig. 26. THD % of the Voltage @ Vb Bus with and without NP-HFC Compensator.

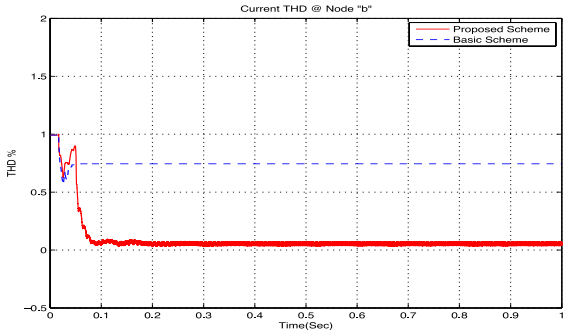

Fig. 27. THD % of the Current @ Vb Bus with and without NP-HFC Compensator.

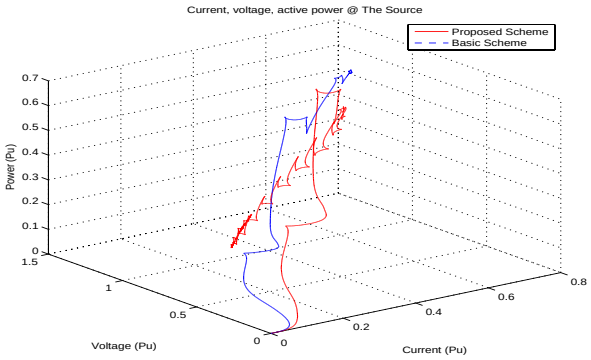

Fig. 28. Current, voltage and active power @ Vs Bus with and without HFC Compensator.

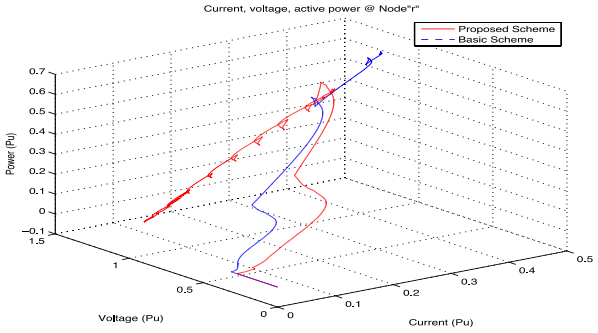

Fig. 29. Current, voltage and active power @ Vr Bus with and without NP-HFC Compensator.

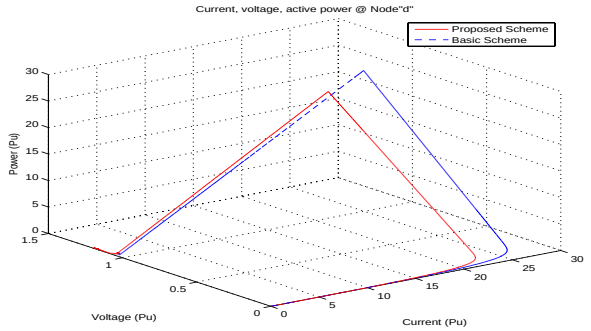

Fig. 30. Current, voltage and active power @ Vd Bus with and without NP-HFC Compensator.

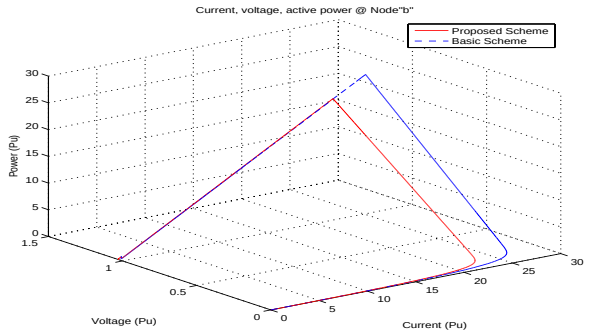

Fig. 31. Current, voltage and active power @ Vb Bus with and without NP-HFC Compensator.

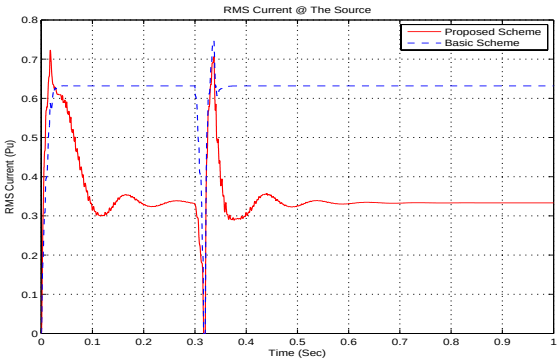

Fig. 32. RMS current Is @ Vs Bus under OC fault with and without NP-HFC Compensator.

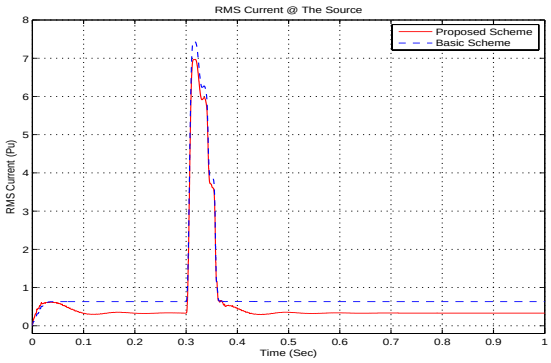

Fig. 36. RMS current Is @ Vs Bus under SC fault with and without NP-HFC Compensator.

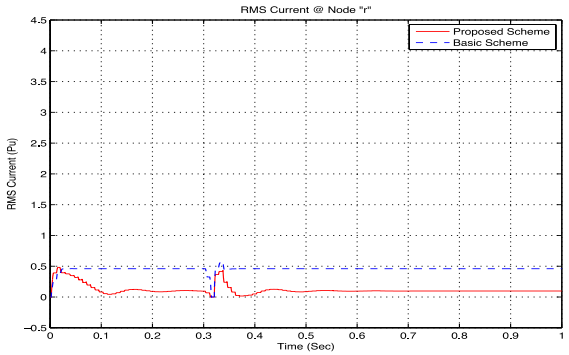

Fig. 33. RMS current Ir @ Vr Bus under OC fault with and without NP-HFC Compensator.

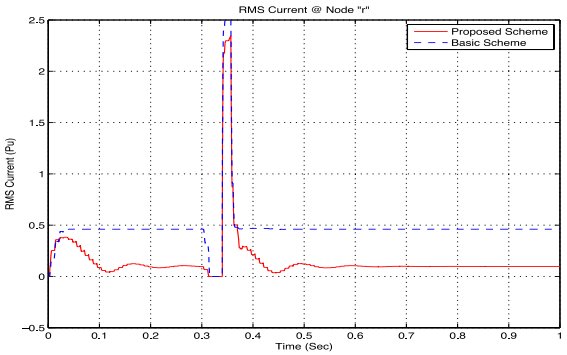

Fig. 37. RMS current Ir @ Vr Bus under OC fault with and without NP-HFC Compensator.

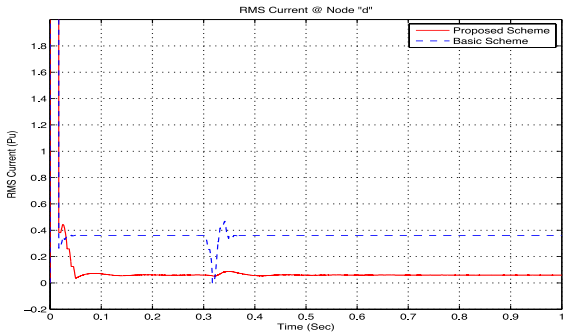

Fig. 34. RMS current Id @ Vd Bus under OC fault with and without NP-HFC Compensator.

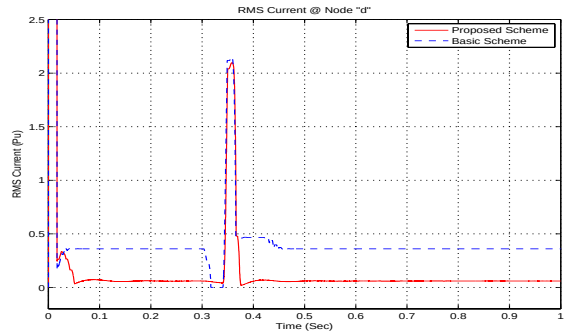

Fig. 38. RMS current Id @ Vd Bus under OC fault with and without NP-HFC Compensator.

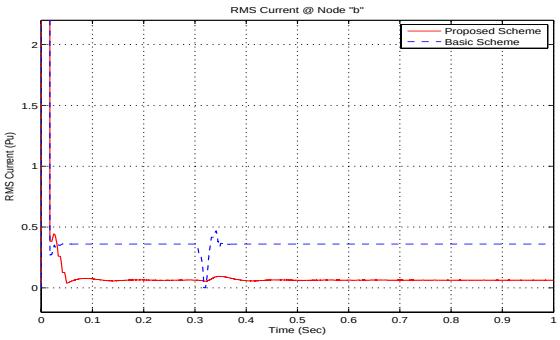

Fig. 35. RMS current Ib @ Vb Bus under OC fault with and without NP-HFC Compensator.

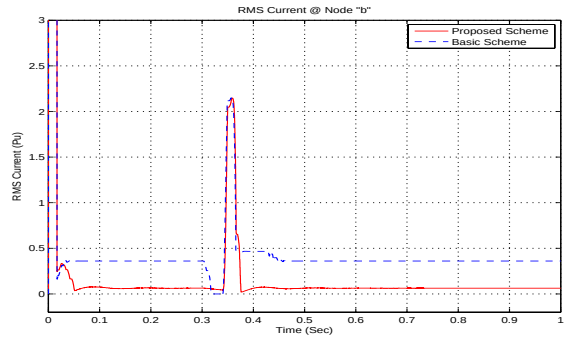

Fig. 39. RMS current Ib @ Vb Bus under SC fault with and without NP-HFC Compensator.

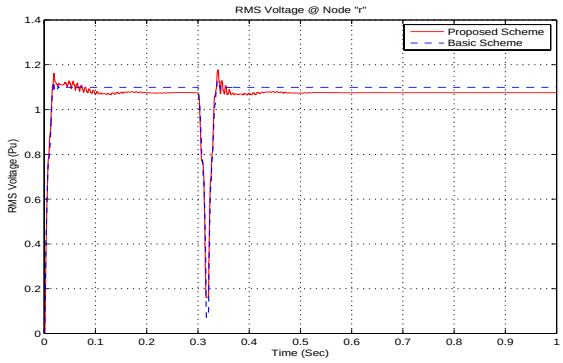

Fig. 40. RMS voltage Vr @ Vr Bus under OC fault with and without NP-HFC Compensator.

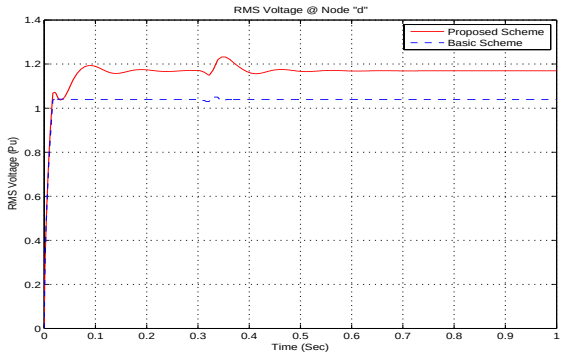

Fig. 41. RMS voltage Vd @ Vd Bus under OC fault with and without NP-HFC Compensator.

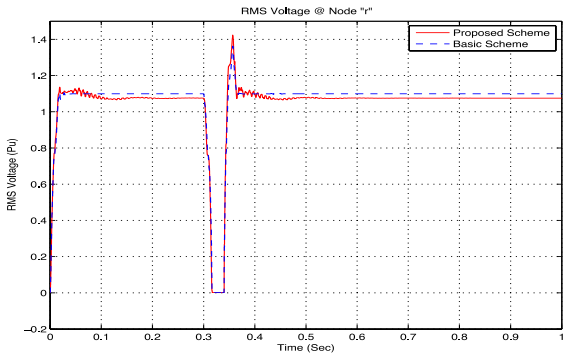

Fig. 42. RMS voltage Vr @ Vr Bus under SC fault with and without NP-HFC Compensator.

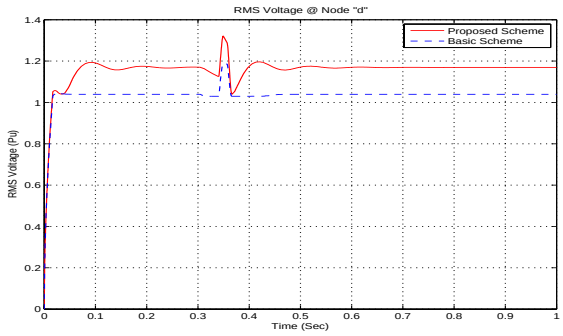

Fig. 43. RMS voltage Vd @ Vd Bus under SC fault with and without NP-HFC Compensator.

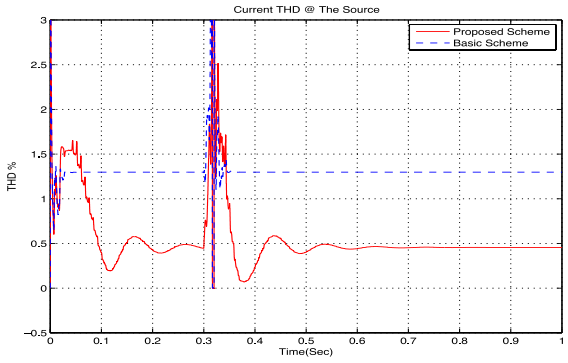

Fig. 44. THD % of the Current @ Vs Bus under OC faul with and without NP-HFC Compensator.

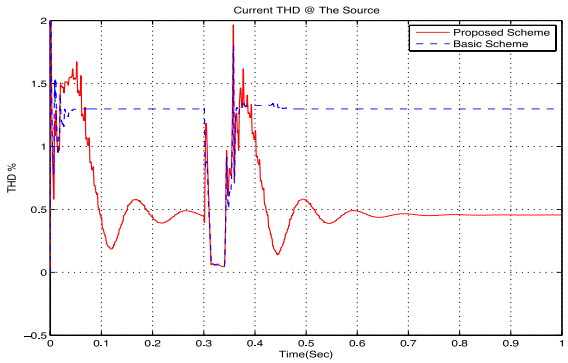

Fig. 45. THD % of the Current @ Vs Bus under SC faul with and without NP-HFC Compensator.

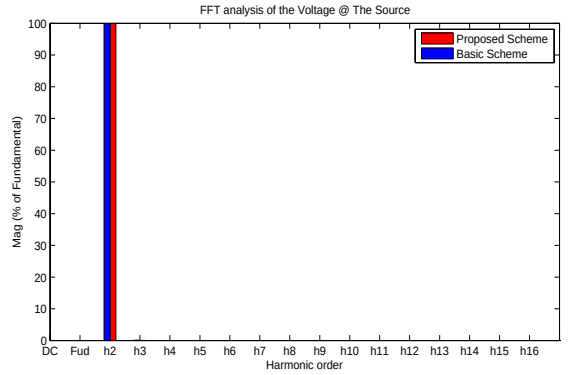

Fig. 46. FFT analysis of the Voltage of the Source with and without the filter Compensator.

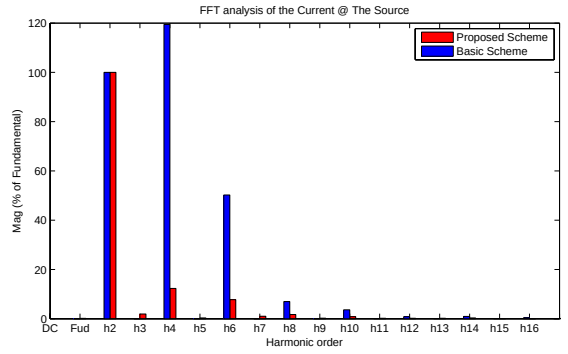

Fig. 47. FFT analysis of the Current of the Source with and without the filter Compensator.

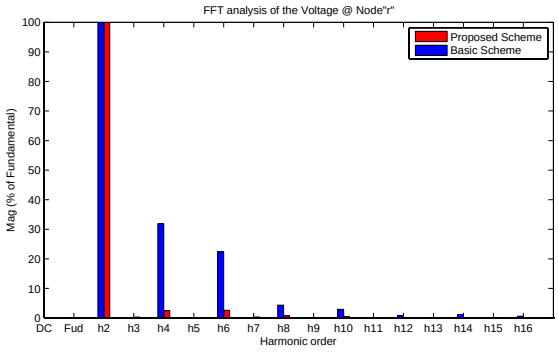

Fig. 48. FFT analysis of the Voltage at node ”R” with and without the filter Compensator.

7. Conclusion

The paper presented the novel FACTS based NP-HFC Filter compensator scheme with an Intercoupled multi-Zonal Target practice error driven error scaled control strategy to ensure AC-DC decoupled operation with improved Power Quality for use inboard/ mobile V2H Battery Charging systems. The FACTS NP-HFC filter compensator can be used in other AC-DC Renewable Energy interface schemes. The FACTS scheme is fully validated using the MATLAB / SIMULINK Software Environment. The common DC Bus scheme feeding the Li-ion Batteryis also stabilzed to ensure stable Buck-Boost converterunder fast charging modesusing the dynamic Pulse Width Modulated switching scheme. The novel V2H battery charger with NP-HFC Filter Compensator can be fitted with other efficient control strategies using error driven multi-loop control strategies with the purpose of damping transient inrush current contions and ensuring voltage regulation at both AC and DC common buses under fastBattery charging modes and short duration open and short circuit conditions. The Li-ion Battery can be rapidly and efficiently charged with the multi-loop error driven dynamic multi regulators intercoupled scheme with the free wheeling energy recovery loop while ensuring energy utilization, improved power factor and enhanced power quality. This ensures fast efficient battery DC source operation. The paper presents a simple Multi-zonal controller equipped with a error-squared scaling for the control of both the DC-DC converter and NP-HFC Hybrid Filter Compensator. The proposed FACTS scheme is validated using the MATLAB / SIMULINK/Sim-power Software Environment.

References

[1] M. Hemphill, “Electricity distribution system planning for an increasing penetration of plug-in electric vehicles in new south wales,” in Universities Power Engineering Conference (AUPEC), 2012 22nd Australasian, Sept. 2012, pp. 1 –6.

[2] A. Rautiainen, C. Evens, S. Repo, and P. Jarventausta, “Requirements for an interface between a plug-in vehicle and an energy system,” in PowerTech, 2011 IEEE Trondheim. IEEE, 2011, pp. 1–8.

[3] R. Tuncay, O. Ustun, M. Yilmaz, C. Gokce, and U. Karakaya, “Design and implementation of an electric drive system for in-wheel motor elec- tric vehicle applications,” in Vehicle Power and Propulsion Conference (VPPC), 2011 IEEE. IEEE, 2011, pp. 1–6.

[4] S. Pang, J. Farrell, J. Du, and M. Barth, “Battery state-of-charge estimation,” in American Control Conference, 2001. Proceedings of the 2001, vol. 2. IEEE, 2001, pp. 1644–1649.

[5] B. Powell and T. Pilutti, “Series hybrid dynamic modeling and control law synthesis,” Ford Scientific Research, TR SR-93-201, 1993.

[6] O. Momoh and M. Omoigui, “An overview of hybrid electric vehicle technology,” in Vehicle Power and Propulsion Conference, 2009. VPPC ’09. IEEE, sept. 2009, pp. 1286 –1292.

[7] J. Tyrus, R. Long, M. Kramskaya, Y. Fertman, and A. Emadi, “Hybrid electric sport utility vehicles,” Vehicular Technology, IEEE Transactions on, vol. 53, no. 5, pp. 1607 – 1622, Sept. 2004.

[8] B. Keogh, “Power factor correction using the buck topologyefficiency benefits and practical design considerations.”

[9] R. Weissbach and K. Torres, “A noninverting buck-boost converter with reduced components using a microcontroller,” in SoutheastCon 2001. Proceedings. IEEE. IEEE, 2001, pp. 79–84.

[10] B. Singh, B. Singh, A. Chandra, K. Al-Haddad, A. Pandey, and D. Kothari, “A review of single-phase improved power quality ac-dc converters,” Industrial Electronics, IEEE Transactions on, vol. 50, no. 5, pp. 962–981, 2003.

[11] F. Musavi, W. Eberle, and W. Dunford, “A high-performance single- phase bridgeless interleaved pfc converter for plug-in hybrid electric vehicle battery chargers,” Industry Applications, IEEE Transactions on, vol. 47, no. 4, pp. 1833–1843, 2011.

[12] E. Elbakush and A. Sharaf, “A hybrid facts pv-smart grid (v2g) battery charging scheme,” International Journal of Advanced Renewable Energy Research, vol. 1, no. 10, pp. 560–572, 2012.

[13] B. Lin, S. Tsay, and M. Liao, “Integrated power factor compensator based on sliding mode controller,” in Electric Power Applications, IEE Proceedings-, vol. 148, no. 3. IET, 2001, pp. 237–244.

[14] E. Elbakush and A. Sharaf,“A low impact-efficient v2h-batterycharging scheme for EV-electric vehicles,” International Journal of Advanced Renewable Energy Research, vol. 1, no. 9, pp. 495–504, 2012.

[15] P. Nandam and P. Sen, “Industrial applications of sliding mode control,” in Industrial Automation and Control, 1995 (I A C’95), IEEE/IAS International Conference on (Cat. No.95TH8005), 5-7jan 1995, pp. 275 –280.

[16] E. Ho and P. Sen, "Control dynamics of speed drive systems using slid- ing mode controllers with integral compensation," Industry Applications, IEEE Transactions on, vol. 27, no. 5, pp. 883–892, 1991.

[17] M. El-Moursi and A. Sharaf, "Novel statcom controllers for voltage stabilisation of wind energy scheme," International journal of global energy issues, vol. 26, no. 3, pp. 382–400, 2006.

[18] A. Sharaf and G. Wang, "Wind energy system voltage and energy enhancement using low cost dynamic capacitor compensation scheme," in Proceedings of the IEEE International Conference on Electrical, Electronic and Computer Engineering, 2004, pp. 804–807.

[19] A. Sharaf and W. Wang, "A low-cost voltage stabilization and power quality enhancement scheme for a small renewable wind energy scheme," in Industrial Electronics, 2006 IEEE International Symposium on, vol. 3. IEEE, 2006, pp. 1949–1953.

[20] H. Chan, "A new battery model for use with battery energy storage systems and electric vehicles power systems," in Power Engineering Society Winter Meeting, 2000. IEEE, vol. 1. IEEE, 2000, pp. 470–475.

[21] B.Kennedy,D.Patterson,andS.Camilleri,"Useoflithiu m-ionbatteries in electric vehicles," Journal of Power Sources, vol. 90, no. 2, pp. 156– 162, 2000.

[22] V. Pop, H. Bergveld, D. Danilov, P. Regtien, and P. Notten, Battery management systems: Accurate state-of-charge indication for battery- powered applications. Springer, 2008, vol. 9.

[23] J. Yen, P. Fan, L. Dung, and F. Shieh, "The prototype implementation of a varying current charger for aged rechargeable lithium-ion batteries," in Consumer Electronics, Communications and Networks (CECNet), 2011 International Conference on. IEEE, 2011, pp. 5421–5424.

[24] S. Bhattacharya, D. Divan, and B. Banerjee, "Control and reduction of terminal voltage total harmonic distortion (thd) in a hybrid series active and parallel passive filter system," in Power Electronics Specialists Conference, 1993. PESC'93 Record., 24th Annual IEEE. IEEE, 1993, pp. 779–786

[25] G. Jung and G. Cho, "New power active filter with simple low cost structure without tuned filters," in Power Electronics Specialists Confer- ence, 1998. PESC 98 Record. 29th Annual IEEE, vol. 1. IEEE, 1998, pp. 217–222.

[26] A. Sharaf and R. Chhetri, "A Novel Dynamic Capacitor Compen- sator/Green Plug Scheme for 3Phase-4 Wire Utilization Loads," in Electrical and Computer Engineering, 2006. CCECE'06. Canadian Conference on. IEEE, 2006, pp. 454–459.

Appendix

Table 2. Parameters of the battery charging system

Device	Value
Battery	Lithium-Ion, 300V, 650Ah, S.O.C 10%
AC Grid	240 V
Cr, Cf	100 μ F
Cd, CB	4500 μ F
Rs, Ro	0.05 Ω
Ls, Lo	0.003 H
γ_{Vr}	1
γ_{Vr_Ripple}	0.5
γ_{Ir}	0.5
γ_{Ir_Ripple}	0.25
K1, K2	0.75, 0.1
γ_{PF}	0.5
γ_{VB}	0.5
γ_{IB}	0.5
γ_{Vd}	1
γ_{Id}	0.5
γ_{Pd}	0.51